ASSOCIATION OF LOCKDOWN POLICIES WITH COVID-19 EARLY CASE GROWTH RATES IN THE UNITED STATES

by

Anna Barefield

A thesis

submitted in partial fulfillment

of the requirements for the degree of

Master of Science in Mathematics

Boise State University

August 2023

BOISE STATE UNIVERSITY GRADUATE COLLEGE

DEFENSE COMMITTEE AND FINAL READING APPROVALS

of the thesis submitted by

Anna Barefield

Thesis Title: Association of Lockdown Policies with COVID-19 Early Case Growth Rates in the United States

Date of Final Oral Examination: 10 April 2023

The following individuals read and discussed the thesis submitted by student Anna Barefield, and they evaluated her presentation and response to questions during the final oral examination. They found that the student passed the final oral examination.

Juna Goo, Ph.D.	Chair, Supervisory Committee
Joe Champion, Ph.D.	Member, Supervisory Committee
Kyungduk Ko, Ph.D.	Member, Supervisory Committee

The final reading approval of the thesis was granted by Juna Goo, Ph.D., Chair of the Supervisory Committee. The thesis was approved by the Graduate College.

Dedicated to Jon and Sandy Barefield

ACKNOWLEDGMENTS

I would like to thank Dr. Juna Goo, as this thesis would not have been possible without her guidance and patience. I would also like to thank the Mathematics Department for financial support through the Summer Research Fellowship.

ABSTRACT

The COVID-19 pandemic has impacted essentially the entire globe, infecting over 755 million people worldwide and resulting in over 6.8 million deaths to date. Different countries have had varying levels of success in managing the spread of the pandemic, and the success or lack thereof could be explained by the impact of government intervention, such as lockdown policies, mask mandates, and social distancing advisories. The United States responded particularly poorly to the early pandemic outbreak as compared to other similar countries, due to its lack of coordinated planning to implement effective policies, with large variations in action taken by each state. Therefore, it is of interest to understand how varying levels of policy implementation are related to early COVID-19 outcomes. In this study, we consider whether the state's emergency declaration was before the national level and the number of other lockdown policies that are in effect on a given day. We also disaggregate the effect of other lockdown policies into between-state and within-state effects. Then we use linear mixed effects model to examine the association between early COVID-19 growth rates and lockdown policies during the initial lockdown period after accounting for statewide demographic variables. Due to multicollinearity issues between demographic variables, we present two final models that account for these variables separately.

TABLE OF CONTENTS

LIST OF TABLES

LIST OF FIGURES

CHAPTER 1

INTRODUCTION

Since its first detection in December 2019 in Wuhan, China, COVID-19 quickly spread to countries worldwide [19]. As of February 9, 2023, the WHO reported over 755 million COVID-19 cases and over 6.8 million COVID-19-related deaths [5]. Given the severity of the situation, many public health experts examined the spread of COVID-19 and the effectiveness of government interventions, such as lockdown policies, mask mandates, and social distancing advisories. A comparative study by Migone [18] found that the effectiveness of containment policies primarily depended on their timing - countries that responded proactively, including Australia, Japan, and South Korea, were less severely impacted by the pandemic, whereas countries that responded reactively, like the United States, suffered more. Dey et al. [8] also noted that U.S. states that responded slowly to the pandemic were generally hit the hardest, likely due to this delayed response in implementing effective policies to contain the spread of COVID-19. Another study by Lee et al. [15] directly compared the government responses of the United States and South Korea. The first case of COVID-19 in the United States and in South Korea was reported on the same day, but South Korea declared a state of emergency on February 23, 2020, whereas the United States did not declare a state of emergency until March 13, 2020. South Korea was able to flatten the curve early on by implementing "swift, decisive" mea-

sures, while the United States "lacked coordinated planning" to effectively implement policies that would curb the growth of COVID-19. These studies demonstrated the importance of coordinated planning to implement policies proactively, and motivated this investigation of the associations between policy implementation and COVID-19 growth rates while taking into account the varied responses taken by each U.S. state.

Many studies have also highlighted health disparities in COVID-19 outcomes related to race, age, gender, and economic status. A county-level analysis by Finch and Finch [9] found that, in the very early stages of the pandemic, counties with higher levels of poverty had more confirmed COVID-19 cases than counties with lower poverty levels, but this relationship flipped after April 1, 2020. Another county-level study by Berman et al. [6] used a generalized linear mixed effects model to analyze socioeconomic predictors of COVID-19 incidence and case fatality rates in Georgia. Berman et al. assumed that the underlying distribution of incidence and case fatality rates followed a Poisson distribution, and therefore a general linear mixed model with log link function was used to examine the relationship between health indicators and COVID-19 outcomes. Berman et al. found that rural county status and higher economic inequality were associated with higher COVID-19 incidence. A study by Pan et al. [19] assessed the epidemiology of the outbreak in Wuhan, China. In this study, Pan et al. divided the study period into 5 groups to examine the dynamics of the epidemic. An epidemic curve was created to show the change of COVID-19 case counts over time and a modified poisson regression with robust variance was used to determine the relationship between COVID-19 rates and age, sex, healthcare occupation, and disease severity (mild and moderate versus severe and critical) by calculating risk ratios. Pan et al. found that the case rate was slightly higher for women than for men, and higher for healthcare workers than for the general population. A

meta-analysis by Mude et al. [24] revealed that the COVID-19 prevalence ratio was significantly higher in Black and Hispanic populations when compared with White population. A study by Hamidi et al. [22] also found that the COVID-19 infection rate was higher in counties with a higher percentage of Black population, and further explored the relationship between county-level activity density (defined as the sum of county population and employment divided by the land area) and COVID-19 case rates in the United States. The study conducted by Hamidi et al. employed a multilevel linear model, which is equivalent to the linear mixed effects model that we used in this study, although we considered the state-level instead of the county-level. This type of model can account for temporal correlations that arise from repeated measurements as well as the nested structure of the data. Hamidi et al. found that, surprisingly, after controlling for confounding variables, including race (percent of Black population), gender (percent of male population), age (percent of population aged 60 and over), education level (percent of adults with education beyond high school), health indicators (percent of adults currently smoking and percent of adults who are overweight), features of a given metropolitan area (metropolitan population and enplanements in metropolitan area per 10,000 population), and healthcare-related features of a given metropolitan area (number of primary care physicians per 10,000 population, state-wide number of COVID-19 testing per 10,000 population, and ICU beds per 10,000 population), higher population density was associated with decreased infection rate. Hamidi et al. noted that this result was at odds with the popular opinion among urban planners that "dense places will experience faster spread of COVID-19" due to increased person-to-person contacts and difficulty with social distancing in these areas, and suggested that "perhaps the heightened attention to social distancing requirements" in compact areas has led to increased compliance

and therefore decreased infection rates. We note that the healthcare-related variables controlled for in the study conducted by Hamidi et al. are not necessarily confounders early in the COVID-19 outbreak, given limited public knowledge about the risks of COVID-19. Other studies of the early outbreak have found population density to be positively related to COVID-19 case rates.

In this study, we focused on the impacts of two different groups of statewide lockdown policies. One type of policy we considered was the state of emergency declaration. To determine if states that acknowledged and responded proactively to the pandemic fared better than states that delayed action, we investigated if whether a state (or the District of Columbia) issued an emergency declaration before or on/after the national emergency declaration date. Other types of policies we considered were policies that required the closure of public spaces, including schools, restaurants and bars, and other non-essential business, as well as stay-at-home orders. Assessing the effect of these lockdown policies presented a challenge in that the number of lockdown policies in place on a given day varied over time. When we considered the number of lockdown policies in place within a given state on a given day, we had information about both between-state differences and within-state differences, and the effects of these differences were confounded. For example, at one level, the number of lockdown policies within a given state changed over time, but at another level, the overall number of lockdown policies varied between states. If the combined "other lockdown policy" variable were treated as a single effect, we could not differentiate between the within-state and between-state effects. As presented by Curran and Bauer [7], the current best practice for disaggregating between-state and within-state effects is person-mean centering, in which the time varying covariate is decomposed into the sum of two parts: the person-level mean, and the time-dependent deviation from

the person-level mean. In the context of our study, the number of other lockdown policies was decomposed into two parts: (1) the mean number of other lockdown policies implemented by a given state during the study period and (2) the amount by which the number of lockdown policies in that state deviated from the mean on a given day. More details about the process of disaggregating between-state and within-state effects are discussed in Section 2.1.1. Another challenge presented by the time-varying covariate (other lockdown policies) was in isolating the effects of the lockdown policies from the effects of the reopening policies that were implemented soon after. Figure 1.1 shows the number of states that implemented new policies on a given day from February 29, 2020 to December 23, 2020. To avoid confounding effects associated with reopening policies, we considered only the period of time between the first confirmed case was reported in the last state the pandemic reached (West Virginia on March 18, 2020, where the growth rate based on the 7-day moving average was defined beginning March 16, 2020) and the date of the first reopening policy (April 20, 2020 in South Carolina, where the study period ended on the previous day, April 19, 2020).

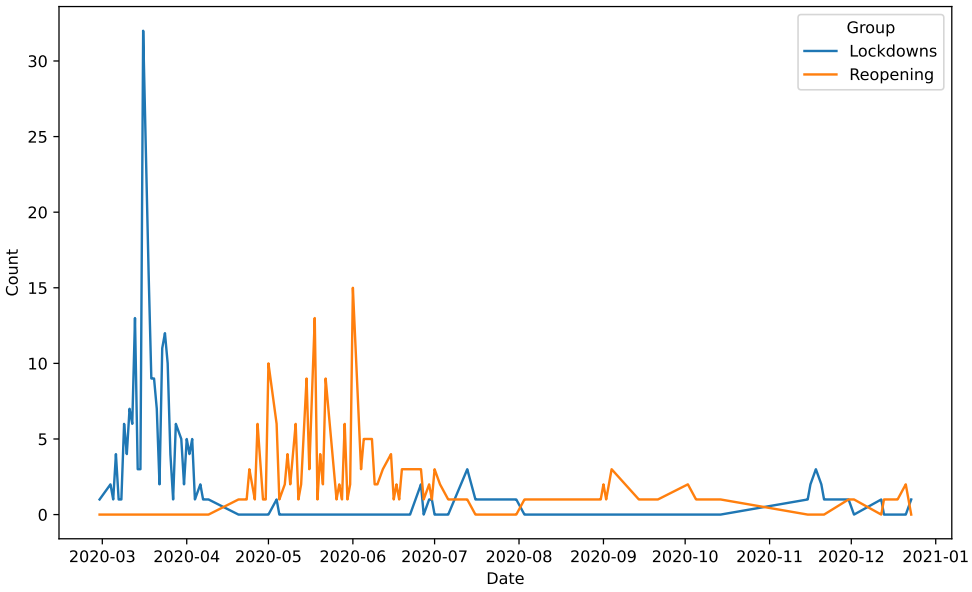

Figure 1.1: The number of states (and the District of Columbia) that implemented new policies on any given date, from February 29, 2020 to December 23, 2020

CHAPTER 2

METHODS

2.1 Data Description

For the COVID-19 case data, we used the Historic US Values data from The Atlantic COVID Tracking Project [3]. We selected the positive variable from the data, defined as the "total number of confirmed plus probable cases of COVID-19 reported by the state or territory". It is important to note that the extent to which the data reflects the actual COVID-19 outbreak is limited in that in early case rates are likely underestimates of the true case rates due to many possible cases going undetected, and that different states use different definitions when reporting confirmed plus probable cases.

The policy data was downloaded from the COVID-19 U.S. State Policy (CUSP) database [20]. The CUSP documents the dates that all 50 states and the District of Columbia implemented policies in response to the COVID-19 pandemic [20]. Specifically, we used the data files titled State of Emergency Declaration, Stay-at-Home Order, and Closures & Reopening. From these datasets, we extracted date data for each of the following policies implemented for each state (and the District of Columbia): emergency declaration, stay-at-home order, school closure, restaurant and bar closure, and other non-essential business closure. For the sake of simplicity, we refer to the 51 regions as states.

We also included state-level demographic variables as covariates in the model. The gender, race/ethnicity, age, poverty, and citizenship status data were reported as proportions of the state population and were obtained from the Kaiser Family Foundation (KFF) [1]. Typically, the KFF data is sourced from the Census Bureau's American Community Survey (ACS), but since the release of the 2020 ACS was delayed due to the COVID-19 pandemic, most of the data reported in 2020 was based on the analysis of the Census Bureau's March Supplement to the Current Population Survey (CPS) [1]. We also considered the population density for each state, which we accessed on the Census Bureau's website. The population density data was based on resident population counts from the 2020 census [2].

2.1.1 Variables

Case Growth Rate The growth rate of confirmed COVID-19 cases was the dependent variable in this study. Considering the raw daily counts of positive COVID-19 cases on a given day j for a given state i, z_{ij}, we calculated the 7-day moving average, m_{ij}, of daily new confirmed cases,

$$m_{ij} = \frac{z_{ij-3} + z_{ij-2} + z_{ij-1} + z_{ij} + z_{ij+1} + z_{ij+2} + z_{ij+3}}{7}$$

and defined the COVID-19 case growth rate by

$$y_{ij} = \frac{m_{ij} - m_{ij-1}}{m_{ij-1}}$$

for $i = 1, \ldots, 51$ and $j = 1, \ldots, 35$.

Time The number of consecutive days since the beginning of the study period, where the value of the time variable is 1 on the first day of the study period, March 16, 2020, and 35 on the last day of the study period, April 19, 2020.

Emergency Declaration The dataset titled "Emergency Declaration" contained data about the dates on which each state declared a state of emergency. From this data, we defined a binary emergency declaration variable so that the variable had a value of 1 if a given state declared a state of emergency before the national emergency declaration date (March 13, 2020) [4], or 0 if the given state declared a state of emergency on or after the national emergency declaration date.

Other Lockdown Policies The dataset titled "Stay-at-Home Order" contained data about the dates on which each state implemented a stay-at-home order, and the dataset titled "Closures & Reopening" contained data about the dates on which each state implemented various policies. We combined data from both datasets, specifically the dates on which the stay-at-home order, school closure, restaurant and bar closure, and other non-essential business closure, were implemented, into a single "other lockdown policy" variable, which we call OLD. This variable is defined as the total number of these lockdown policies in place on a given day in a given state. For example, Idaho issued its first lockdown policy, namely K-12 public school closure, on March 24, and implemented the remaining "other lockdown policies" - stay-at-home order, restaurant and bar closure, and other non-essential business closure - on March 25. Therefore the value of the OLD variable for Idaho is 0 from March 16 through March 23, 1 on March 24, and 4 from March 25 through the end of the study period, April 19.

Since the measurement of the OLD variable is repeated, it contains information about both the within-state effect and the between-state effect [14]. To disaggregate within- and between-state effects, one can use state-mean centering as follows:

$$COLD_{ij} = OLD_{ij} - MOLD_i.$$

where $COLD_{ij}$ is the number of additional lockdowns in effect on a given jth day, based on the average for the ith state over the study period and $MOLD_i$ is the average number of other lockdown policies for the ith state. We consider

$$\begin{aligned}
&\text{Level 1: } y_{ij} = \beta_{0i} + \beta_1 COLD_{ij} + \beta_2 MOLD_i + \varepsilon_{ij} \\
&\text{Level 2: } \beta_{0i} = \gamma_{00} + u_{0i} \\
&\qquad\qquad \beta_1 = \gamma_{01} \\
&\qquad\qquad \beta_2 = \gamma_{11}.
\end{aligned}$$

Then

$$y_{ij} = \gamma_{00} + \gamma_{01} COLD_{ij} + \gamma_{11} MOLD_i + u_{0i} + \varepsilon_{ij}$$

where $u_{0i} \overset{i.i.d}{\sim} N(0, \sigma_u^2)$, $\varepsilon_{ij} \overset{i.i.d}{\sim} N(0, \sigma_e^2)$, and γ_{00}, γ_{01} and γ_{11} are fixed. γ_{01} is the within-state effect, and γ_{11} is the between-state effect. In this case, we can test whether the effects within and/or between states are statistically significant and whether the two effects conflict based on the signs of the coefficients.

Demographic Variables We considered gender, race/ethnicity, age, and poverty and citizenship status as covariates in the model. This data was downloaded from the

Kaiser Family Foundation Population and People in Poverty (2020 Current Population Survey), and is reported at the state level [1]. In particular, we used the tables "Population Distribution by Sex (CPS)" for the Female variable (Female proportion of state population), "Population Distribution by Race/Ethnicity (CPS)" for the Black variable (Black proportion of state population), "Population Distribution by Age (CPS)" for the Over65 variable (the proportion of state population over the age of 65), "Distribution of Total Population by Federal Poverty Level (CPS)" for the P399 variable (the proportion of households in the state which have a total income from 200-399% of the poverty line) , and "Population Distribution by Citizenship Status (CPS)" for the Noncitizen variable (Non-citizen proportion of state population). Some missing values in the Non-Citizen variable were imputed by subtracting Citizen proportion of state population from 1.

We also considered the population density data, which was extracted from the Historical Apportionment File on the Census Bureau's website. The population density is defined as the average population per square mile of land for each state [2]. Since there is extreme variability among state population density values, the smallest being 1.3 in Alaska and the largest being $11,280$ in the District of Columbia, we used the natural logarithm of the population density in our model. We refer to this variable as Density.

2.2 Linear Mixed Model

Our data exhibits dependency as repeated measured COVID-19 growth rates and policies over time are clustered at the state level. Since the existence of dependence violates the assumptions of simple linear regression, it is ideal to use a model that takes

into account both the hierarchical nature of the data and the temporal correlation that arises from repeated measures, such as a linear mixed effects model (also known as a multilevel model). The linear mixed model is given by the equation

$$\boldsymbol{y} = \boldsymbol{X}\boldsymbol{\beta} + \boldsymbol{Z}\boldsymbol{u} + \boldsymbol{e} \tag{2.1}$$

where $\boldsymbol{y}$ is a $N \times 1$ response vector of repeated measurements for each cluster i ($i = 1, \ldots, n$), $N = \sum_{i=1}^{n} m_i$, where m_i is the size of the ith cluster, $\boldsymbol{X}$ and $\boldsymbol{Z}$ are, respectively, $N \times p$ and $N \times q$ fixed and known matrices called design matrices, $\boldsymbol{\beta}$ is a $p \times 1$ vector of p unknown fixed effects parameters, $\boldsymbol{u}$ is a $q \times 1$ vector of q unknown random effects parameters, and $\boldsymbol{e}$ is a $N \times 1$ random error vector. We assume that $\boldsymbol{u}$ and $\boldsymbol{e}$ are normally distributed with mean of a zero vector and

$$\text{Var} \begin{bmatrix} \boldsymbol{u} \\ \boldsymbol{e} \end{bmatrix} = \begin{bmatrix} \boldsymbol{G} & \boldsymbol{0} \\ \boldsymbol{0} & \boldsymbol{R} \end{bmatrix}$$

where $\boldsymbol{G}$ is the variance-covariance matrix of the random effects and $\boldsymbol{R}$ is the variance-covariance matrix of the residuals [16]. In contrast with the simple linear model, which includes only fixed effects, the mixed model allows for both fixed and random effects by including terms $\boldsymbol{X}\boldsymbol{\beta}$ for fixed effects and $\boldsymbol{Z}\boldsymbol{u}$ for random effects.

Henderson [13] developed a set of equations that allow us to simultaneously estimate parameters $\boldsymbol{\beta}$ and $\boldsymbol{u}$. Henderson originally derived these equations by maximizing the joint density of $\boldsymbol{y}$ and $\boldsymbol{u}$ with respect to $\boldsymbol{\beta}$ and $\boldsymbol{u}$, assuming that $\boldsymbol{u}$ and $\boldsymbol{e}$ are normally distributed. These are known as Henderson's Mixed Model Equations (MME), and are commonly presented in the matrix form shown below [21].

$$\begin{bmatrix} \boldsymbol{X'R^{-1}X} & \boldsymbol{X'R^{-1}Z} \\ \boldsymbol{Z'R^{-1}X} & \boldsymbol{Z'R^{-1}Z + G^{-1}} \end{bmatrix} \begin{bmatrix} \hat{\boldsymbol{\beta}} \\ \hat{\boldsymbol{u}} \end{bmatrix} = \begin{bmatrix} \boldsymbol{X'R^{-1}y} \\ \boldsymbol{Z'R^{-1}y} \end{bmatrix} \tag{2.2}$$

Solving for $\hat{\boldsymbol{\beta}}$ and $\hat{\boldsymbol{u}}$, we can write the solutions to Henderson's MME as follows: [16]

$$\hat{\boldsymbol{\beta}} = \left(\boldsymbol{X'V^{-1}X}\right)^{-1} \boldsymbol{X'V^{-1}y} \tag{2.3}$$

$$\hat{\boldsymbol{u}} = \boldsymbol{GZ'V}^{-1} \left(\boldsymbol{y - X\hat{\beta}}\right) \tag{2.4}$$

where $\boldsymbol{V = ZGZ' + R}$. The solutions to Henderson's Model Equations are known as the the BLUE (best linear unbiased estimator) of $\boldsymbol{\beta}$ and the BLUP (best linear unbiased predictor) of $\boldsymbol{u}$ [16]. These estimators are "best" in that they minimize mean squared error (compared with other linear unbiased estimators), "linear" in that they are linear functions of $\boldsymbol{y}$, and "unbiased" in that $E(\hat{\boldsymbol{\beta}}) = \beta$ and $E(\hat{\boldsymbol{u}}) = u$. Now, we call $\hat{\boldsymbol{\beta}}$ an "estimator" because it estimates fixed effects, and we call $\hat{\boldsymbol{u}}$ a "predictor" because it is an estimator for a random effect [21].

In deriving the BLUE and BLUP, $\boldsymbol{G}$ and $\boldsymbol{R}$ were considered to be known. However, in practice, $\boldsymbol{G}$ and $\boldsymbol{R}$ are often unknown and must be estimated. Estimates $\hat{\boldsymbol{G}}$ and $\hat{\boldsymbol{R}}$ are obtained and plugged in to the mixed-model equations to yield estimates of $\hat{\boldsymbol{\beta}}$ and $\hat{\boldsymbol{u}}$, at which point we call the estimates the EBLUE and EBLUP, for "emperical" or "estimated" BLUE and BLUP [16]. There are four approaches to estimating covariance parameters: Analysis of Variance (ANOVA), Maximum Likelihood (ML), and Restricted Maximum Likelihood (REML) and Bayesian approach. In this study, we only consider ML and REML approaches. The ML approach for estimating covariance parameters involves maximizing the marginal log-likelihood function of $\boldsymbol{y}$ with respect to $\boldsymbol{\beta}$ and $\boldsymbol{\theta}$, where $\boldsymbol{\theta}$ is a vector of covariance parameters from which

$\boldsymbol{G}$ and $\boldsymbol{R}$ can be constructed [16]. A shortcoming of the ML estimator, however, is the fact that the ML estimates of the variance components are biased downwards as they fail to take into account the degrees of freedom lost in the estimates of the fixed effects [11]. The REML method aims to resolve this issue by maximizing the log-likelihood of $\boldsymbol{Ky}$, where $\boldsymbol{K}$ is a matrix of error contrasts, so that the likelihood function can be expressed without reference to fixed effects $\boldsymbol{\beta}$. REML is the default method for estimating covariance parameters in many statistical packages. However, as noted in [12], comparing models with different fixed effects is not valid for models fitted by REML, so the ML method is used when testing fixed effects between models, and once the fixed effects are determined, the model is re-fitted with the REML method for unbiased variance estimation.

2.2.1 SAS PROC MIXED

Linear Mixed Model in SAS The MIXED procedure in SAS has made accessible the use of the linear mixed model in research. Using only a few statements, we can specify all that is needed to fit a linear mixed model. The models created for this study are implemented as follows: First, a CLASS statement is used to specify classification or categorical variables used in the model. The classification variables used in our study include the states, the binary emergency declaration variable, and the time variable (indicating 35 consecutive days). Next, a MODEL statement is used to indicate the fixed effects that will be included in the model. Within the MODEL statement, we can also choose a method for computing degrees of freedom for calculating F-statistics for fixed effects, which we must include in this study since the default method fails to take into account complexities introduced by complex covariance structures [16], as discussed further below. Next, a RANDOM statement

is used to indicate the random effects that should be included in the model. We also indicate the subjects (states) and the $\boldsymbol{G}$ (between-state) covariance structure in the RANDOM statement. In this study, we consider random intercept models. Thus, $\boldsymbol{G}$ is a scalar with represents the variance for the random intercept. Finally, a REPEATED statement is used to specify the variable on which we have repeated measures, in our case, time. Like in the RANDOM statement, we also include the subject in this statement, along with the $\boldsymbol{R}$ (within-state) covariance structure. For 35 consecutive measurements for a given state, $\boldsymbol{R}$ is a 35×35 matrix. The MIXED procedure allows for estimating many different possible covariance structures, a few of which are described in the following paragraph. The SAS code used to produce each model used in this study is presented in Appendix A.

Covariance Structure By default, the MIXED procedure uses the variance components (VC) covariance structure to estimate covariance parameters for $\boldsymbol{G}$ and $\boldsymbol{R}$, but this structure is too simple to accurately represent the data, as it assumes no correlation between random effects ($\boldsymbol{G}$) and between repeated measures ($\boldsymbol{R}$), respectively. As repeatedly measured COVID-19 growth rates are expected to be correlated, it is more plausible to specify a covariance structure that allows for correlations, such as compound symmetry (CS) and first-order autoregressive (AR(1)). Compound symmetry allows for correlated errors, but requires that these correlations be the same for all time lags. The first-order autoregressive structure also allows for correlated errors, but requires that these correlations decline exponentially over time, so that correlations are larger between observations taken at closer points in time than correlations between observations taken at distant points in time. While these covariance structures are less restrictive than the variance components structure, they

are still somewhat restrictive in the sense that they are homogeneous structures, meaning that they require the variances along the main diagonal to be constant [26]. To allow for more flexibility in the covariance structure, we also considered some heterogeneous structures in order to estimate G and R. Two such structures are the heterogeneous compound symmetry (CSH) and the heterogeneous first-order autoregressive structure (ARH(1)), which are analogous to the homogeneous CS and AR(1) structures, respectively, but are more general in that they allow the variances along the main diagonal to vary [26]. There exist even more general covariance structures, like first-order ante-dependence (ANTE(1)), which is a generalization of ARH(1), and unstructured (UN), which is the most general as it allows for unique values for all correlations [26].

Denominator Degrees of Freedom In PROC MIXED, the default method for calculating degrees of freedom when a RANDOM statement is specified is the "containment" method. However, this method only provides exact denominator degrees of freedom when there is no $\mathbf{R}$ covariance structure, or in the case that we assume independent and identically distributed errors [23]. Guerin and Stroop [10] showed that using the default method for calculating denominator degrees of freedom leads to inflated type I error rates, especially for models with complex covariance structures. Two common alternative methods for approximating denominator degrees of freedom are the Kenward-Rogers method (df=KR) and Satterthwaite method (df=Sat). The Satterthwaite method can be applied to both models fitted using ML and REML, while the Kenward-Rogers method is only applied to REML models [17]. For models with complex covariance structures, like the one we present, it is recommended that the Kenward-Rogers is used for models fitted using REML [23]. In this study, we

used the Satterthwaite method with models fitted using ML, and the Kenward-Rogers method with models fitted using REML.

CHAPTER 3

RESULTS

Using the COVID-19 case growth rate as described in 2.1.1, we created growth curves for each US state over the study period, which are shown in Figure 3.1. We see that the COVID-19 growth rates generally decreased over time at varying rates across states. The baseline growth rate on the first day of the study period (March 16, 2020) varies between states. The differences between baseline growth rates is partially a result of how the study period was defined. We began the study period on the first day that the COVID-19 growth rate was defined for all states, so since West Virginia reported its first COVID-19 case on March 18, 2020 [3], we began the study period on March 16, 2020. So the baseline growth rate does not represent the initial growth rate for all states. For example, Washington reported its first COVID-19 case on January 19, 2020 [3], so its baseline growth rate represents the COVID-19 growth rate nearly two months after its initial exposure. The mixed-effects model allows us to account for these between-state baseline differences by allowing each state to have its own intercept, normally distributed around 0 with some unknown variance. Each model we created includes a random intercept term to allow for this. We also considered a random slope model that allowed the slope of the COVID-19 growth rate over time to vary for each state, but the $\boldsymbol{G}$ matrix was not positive definite for this model, indicating that there was not much variation in the slope between states.

First, the full model includes all variables that we considered. These variables are: ED, Time, COLD, MOLD, Female, Black, P399, Density, Over65 and Noncitizen. Figure 3.2 shows the variable values by state for the time-invariant covariates (all variables except for Time and COLD). In addition to these variables alone, the full model will include interaction effects between ED and Time, ED and COLD, and ED and MOLD. We fixed the covariance structures $\boldsymbol{G}$ as unstructured (UN), and $\boldsymbol{R}$ as heterogeneous autoregressive (ARH(1)). The specification of the covariance structure $\boldsymbol{G}$ is important when more than one random effect is involved, but since we only consider the random intercept model, $\boldsymbol{G}$ is simply the variance of the random intercept. We chose ARH(1) for $\boldsymbol{R}$ since it assumes that the correlations between within-state residuals decrease exponentially over time and allows for heterogeneous variances.

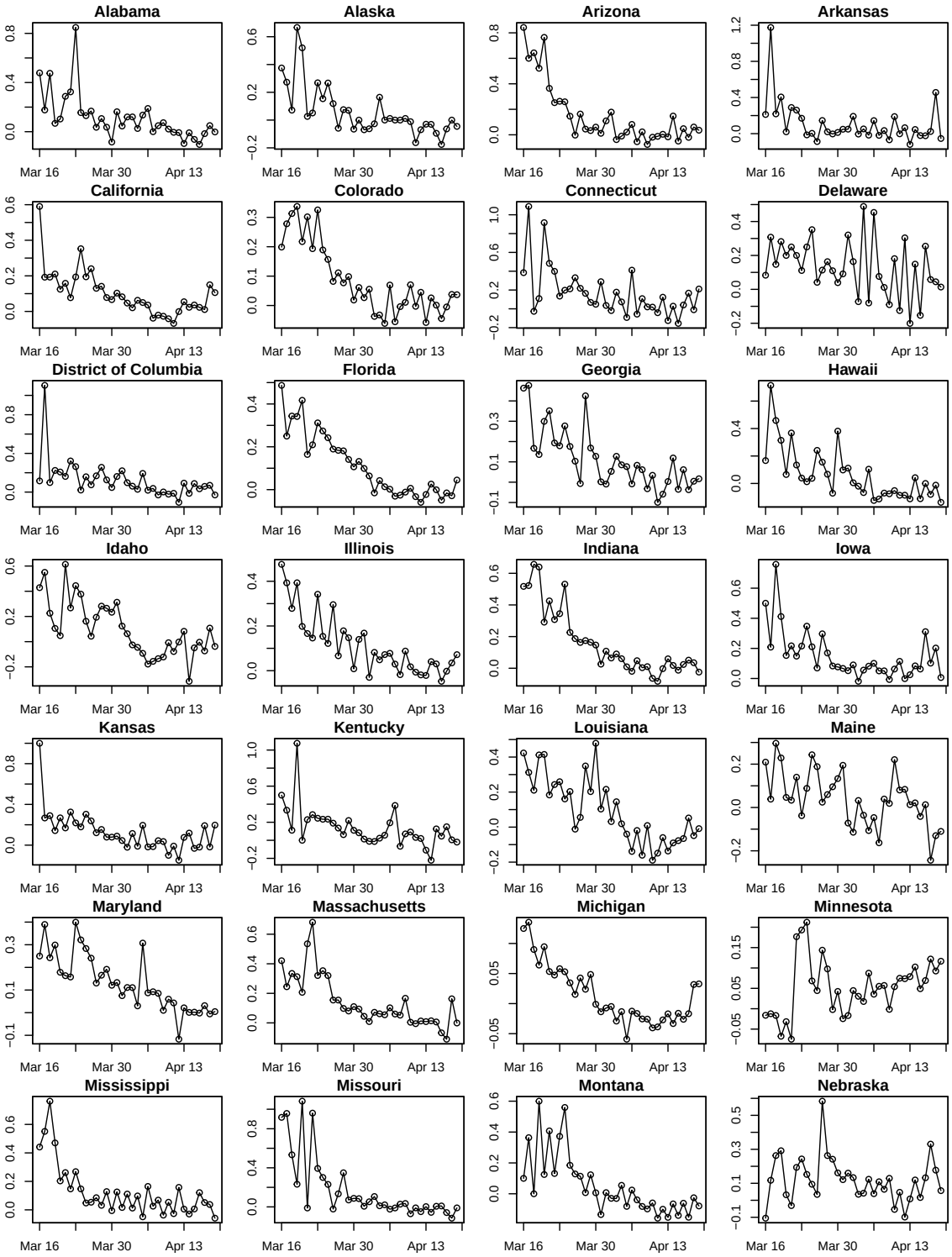

Figure 3.1: Growth Curves

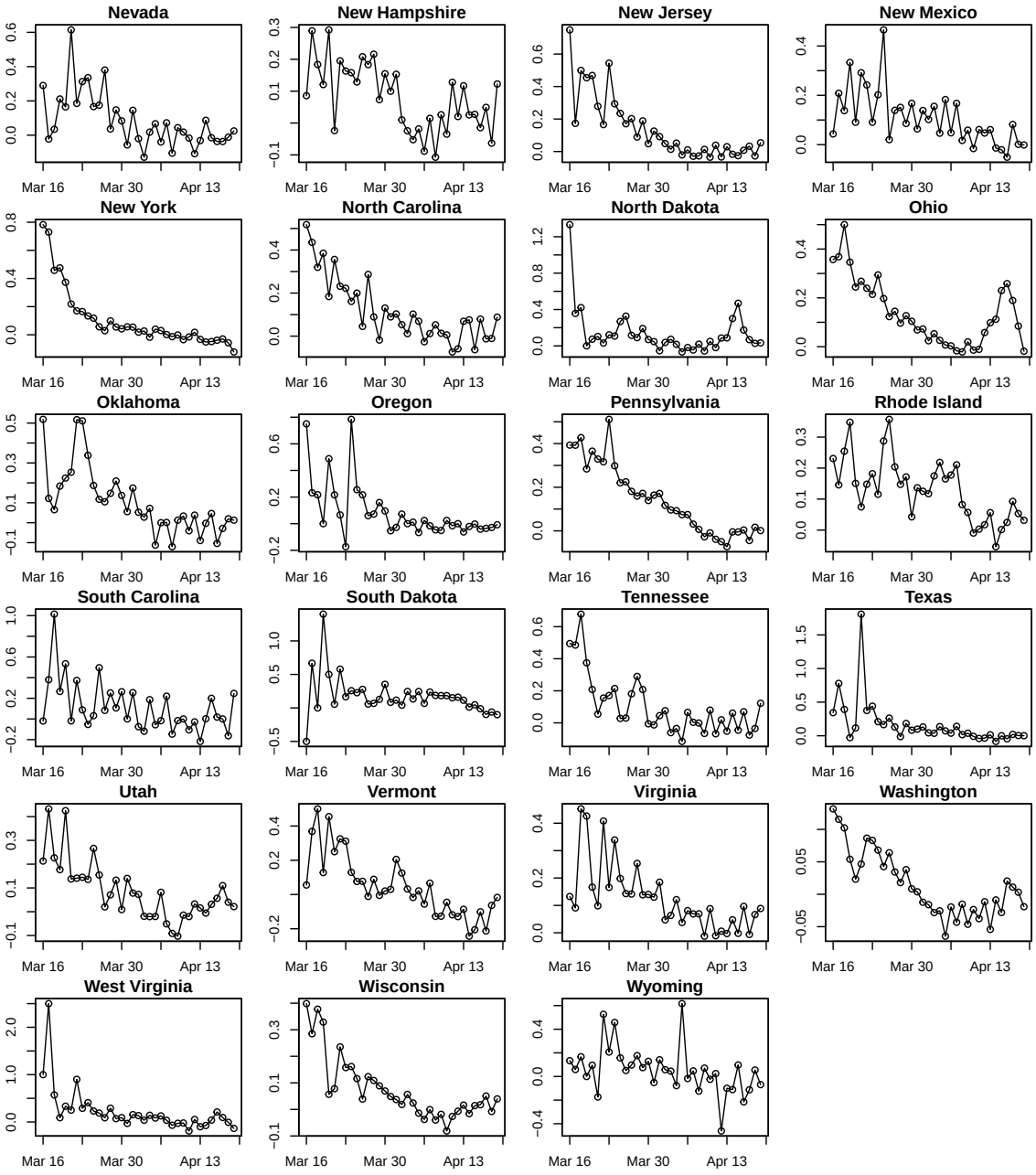

Figure 3.1: Growth Curves (cont.)

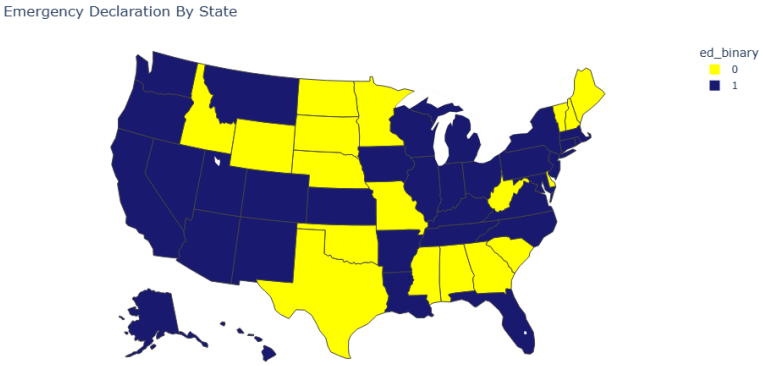

(a) ED

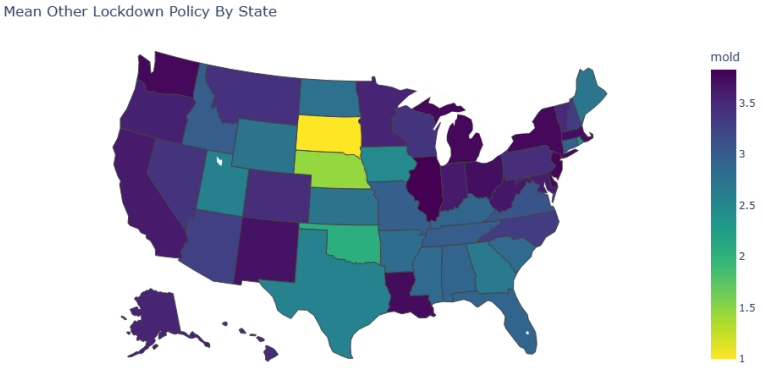

(b) MOLD

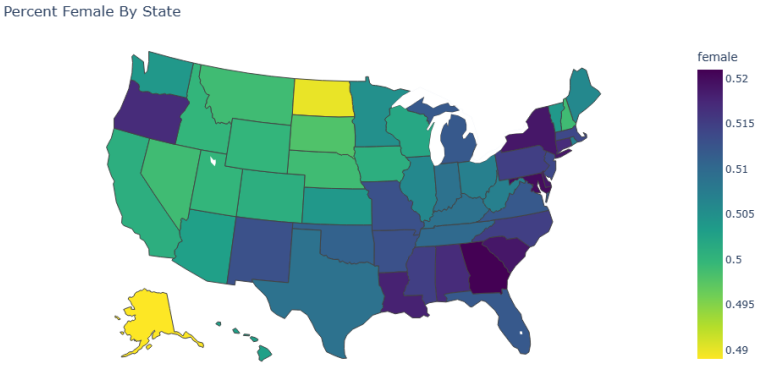

(c) Female

Figure 3.2: Variables by State

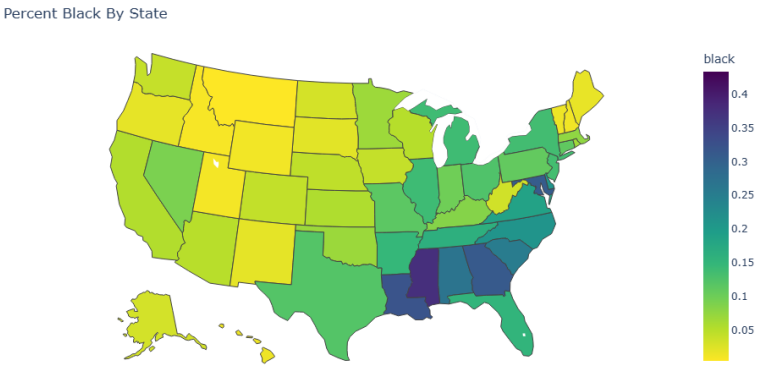

(d) Black

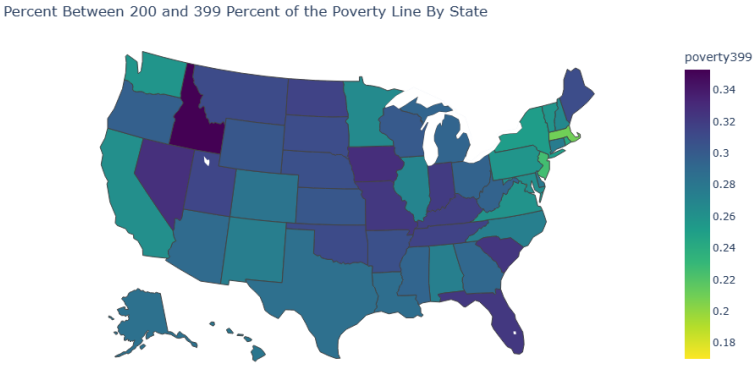

(e) Poverty399

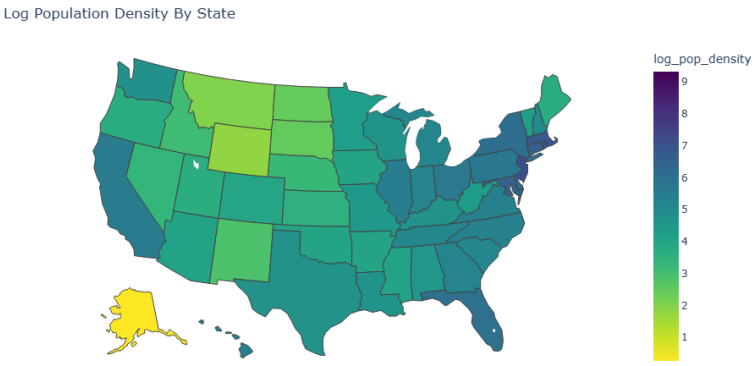

(f) Density

Figure 3.2: Variables by State (cont.)

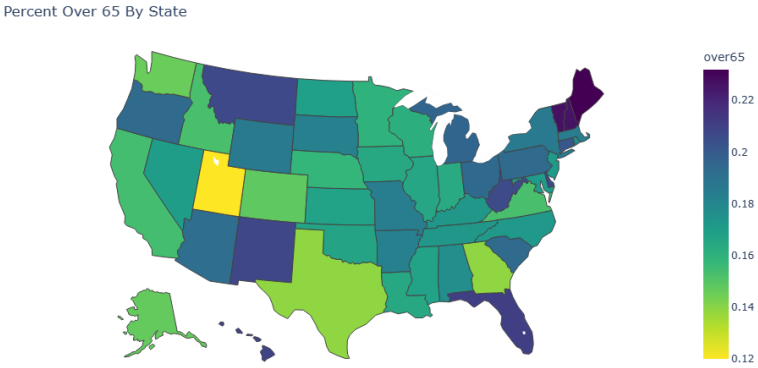

(g) Over65

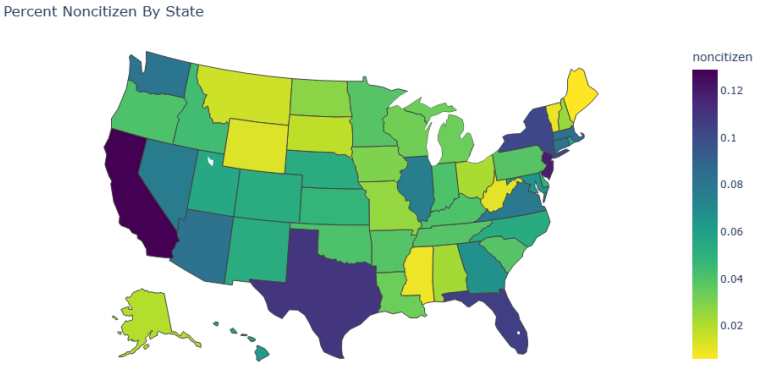

(h) Noncitizen

Figure 3.2: Variables by State (cont.)

3.1 Model Selection

As shown in Table 3.1, some of the variables included in the model are highly correlated, in particular, the correlation between the Female and Black variable is 0.7226, and the correlation between the Female and Density variable is 0.6631. When ignoring the correlation between the deomgraphic variables, Table 3.2 shows the estimates of fixed effects for the full model fitted by three different methods: a

multiple linear regression with ordinary least squares estimation (OLS) and linear mixed effects models with ML and REML, respectively.

Table 3.1: Covariates: Pearson Correlation Matrix

	Female	Black	P399	Density	Over65	Noncitizen
Female	1.0000	0.7226	-0.3413	0.6631	0.0990	0.2129
Black	0.7226	1.0000	-0.3195	0.5405	-0.2523	0.0898
P399	-0.3413	-0.3195	1.0000	-0.6310	0.0762	-0.3514
Density	0.6631	0.5405	-0.6310	1.0000	-0.0063	0.4790
Over65	0.0990	-0.2523	0.0762	-0.0063	1.0000	-0.2919
Noncitizen	0.2129	0.0898	-0.3514	0.4790	-0.2919	1.0000

Table 3.2: Estimates of Fixed Effects in the Full Model

	OLS			ML			REML		
Effect	Est.	S.E.	p-value	Est.	S.E.	p-value	Est.	S.E.	p-value
Intercept	-0.1490	0.4131	0.7184	0.2513	0.3953	0.5278	0.2524	0.4508	0.5787
ED	-0.0199	0.0540	0.7124	0.0101	0.0507	0.8431	0.0098	0.0573	0.8654
Time	-0.0080	0.0006	<.0001	-0.0071	0.0007	<.0001	-0.0071	0.0007	<.0001
ED*Time	-0.0001	0.0011	0.8975	0.0005	0.0009	0.5533	0.0005	0.0009	0.5455
COLD	-0.0538	0.0080	<.0001	-0.0260	0.0071	0.0003	-0.0255	0.0075	0.0007
ED*COLD	0.0149	0.0118	0.2080	-0.0229	0.0104	0.0276	-0.0236	0.0109	0.0302
MOLD	-0.0269	0.0129	0.0368	-0.0315	0.0092	0.0013	-0.0316	0.0105	0.0046
ED*MOLD	0.0087	0.0157	0.5775	-0.0048	0.0150	0.7509	-0.0048	0.0171	0.7806
Female	0.7726	0.8655	0.3721	0.1348	0.8285	0.8714	0.1355	0.9451	0.8867
Black	-0.0104	0.0648	0.8722	-0.0002	0.0620	0.9973	-0.0002	0.0707	0.9983
P399	0.1987	0.1635	0.2243	-0.0876	0.1566	0.5783	-0.0898	0.1786	0.6178
Density	0.0094	0.0047	0.0454	0.0069	0.0045	0.1302	0.0068	0.0051	0.1879
Over65	-0.0581	0.1989	0.7702	-0.0840	0.1904	0.6610	-0.0833	0.2172	0.7035
Noncitizen	0.1163	0.1730	0.5015	0.0448	0.1655	0.7879	0.0453	0.1888	0.8117

The estimates using ML (with df=Sat) and REML (with df=KR) are similar, but the estimates using OLS are not. For example, the OLS estimates differ in sign from

both the ML and REML estimates for the Intercept, ED, ED*Time, ED*COLD, ED*MOLD, and P399. Now, to avoid multicollinearity issues, we considered these highly correlated variables separately in two different models: Model A, which includes ED, Time, COLD, MOLD, Female, P399, Over65, and Noncitizen, and Model B, which includes ED, Time, COLD, MOLD, Black, P399, Density, Over65, and Noncitizen. We also included three interaction effects: one between ED and Time to investigate if the trajectories of COVID-19 growth rates over time were different depending on whether the state declared a state of emergency before or on/after the national emergency, one between ED and COLD to investigate if the within-state impact of other lockdown policies on COVID-19 growth rates depended on whether the state declared a state of emergency before or on/after the national emergency, and one between ED and MOLD to investigate if the between-state impact of other lockdown policies on COVID-19 growth rates depended on whether the state declared a state of emergency before or on/after the national emergency.

3.1.1 Fixed Effects

We began with the full Model A, as described above. Again, we considered covariance structures $\boldsymbol{G}$ as UN and $\boldsymbol{R}$ as ARH(1). We then removed insignificant fixed effects one by one in a method like backward elimination. Unlike traditional backward elimination that removes the effect with the least significant F statistic, we first eliminated insignificant interaction effects. As a result, ED*MOLD and ED*Time were removed in both models A and B. Since ED*COLD was statistically significant, we kept the corresponding main effects ED and COLD regardless of their significance due to the interpretation of the interaction effect in the presence of main effects in the model. Next, we removed the demographic variable with the highest p-value one

at a time while keeping policy variables in the model. We then selected the best final model using a likelihood-ratio test. As noted in [12], comparing models with different fixed effects is not valid for models fitted by REML. For all likelihood ratio tests, the likelihoods were based on ML rather than REML, the default method used by PROC MIXED. At $\alpha = 0.1$, the model including Female and P399 as covariates was preferred over the model including only Female as a covariate ($p = 0.069$). The final Model A includes variables ED, Time, COLD, MOLD, Female, and P399, and the interaction effect between ED and COLD. While neither Female nor P399 is significant at $\alpha = 0.05$ in the final model, it is important to note that the the p-value does not measure the size of an effect or the importance of a result, so scientific conclusions and business policy decisions should not be based only on whether a p-value passes a specific threshold [25]. For Model B, the likelihood ratio test indicated that adding the Black and P399 covariates to the model that included only Density as a covariate did not significantly improve the model, so we chose the final Model B to include the variables ED, Time, COLD, MOLD, Density, and the interaction effect between ED and COLD. Both Over65 and Noncitizen effects were insignificant even when considered as the only demographic variable in the model. Table 3.3 shows the effect estimates through the backward elimination process. The models fix ARH(1) covariance structure for $\boldsymbol{R}$, and are fitted using ML.

Table 3.3: Fixed Effects Estimates ARH(1) (ML)

(a) Model A

	Full	Reduced 1	Reduced 2	Reduced 3	Reduced 4
Intercept	-0.0121 (0.2677)	-0.0103 (0.2693)	-0.0220 (0.2681)	-0.0174 (0.2679)	-0.0330 (0.2697)
ED	0.0336 (0.0491)	-0.0032 (0.0191)	0.0070 (0.0099)	0.0074 (0.0098)	0.0107 (0.0092)
Time	-0.0071*** (0.0007)	-0.0072*** (0.0007)	-0.0068*** (0.0004)	-0.0068*** (0.0004)	-0.0068*** (0.0004)
ED*Time	0.0005 (0.0009)	0.0005 (0.0009)			
COLD	-0.0257*** (0.0071)	-0.0254*** (0.0071)	-0.0277*** (0.0062)	-0.0276*** (0.0062)	-0.0275*** (0.0062)
ED*COLD	-0.0236* (0.0104)	-0.0235* (0.0104)	-0.0199* (0.0086)	-0.0200* (0.0086)	-0.0202* (0.0086)
MOLD	-0.0299** (0.0094)	-0.0343*** (0.0077)	-0.0342*** (0.0077)	-0.0348*** (0.0075)	-0.0356*** (0.0075)
ED*MOLD	-0.0119 (0.0146)				
Female	0.7666 (0.5099)	0.7793 (0.5124)	0.7869 (0.5113)	0.7643 (0.5067)	0.8277 (0.5067)
P399	-0.2246 (0.1349)	-0.2120 (0.1346)	-0.2098 (0.1343)	-0.2142 (0.1338)	-0.2467 (0.1306)
Over65	-0.0590 (0.1615)	-0.0515 (0.1623)	-0.0528 (0.1619)		
Noncitizen	0.1330 (0.1477)	0.1214 (0.1479)	0.1222 (0.1477)	0.1345 (0.1428)	

(b) Model B

	Full	Reduced 1	Reduced 2	Reduced 3	Reduced 4	Reduced 5
Intercept	0.3147*** (0.0648)	0.3157*** (0.0648)	0.3079*** (0.0634)	0.3008*** (0.0612)	0.3031*** (0.0611)	0.2697*** (0.0221)
ED	0.0096 (0.0506)	-0.0050 (0.0189)	0.0047 (0.0097)	0.0056 (0.0096)	0.0068 (0.0092)	0.0062 (0.0091)
Time	-0.0071*** (0.0007)	-0.0071*** (0.0007)	-0.0068*** (0.0004)	-0.0068*** (0.0004)	-0.0068*** (0.0004)	-0.0068*** (0.0004)
ED*Time	0.0005 (0.0009)	0.0005 (0.0009)				
COLD	-0.0259*** (0.0071)	-0.0259*** (0.0071)	-0.0280*** (0.0062)	-0.0279*** (0.0062)	-0.0279*** (0.0061)	-0.0280*** (0.0061)
ED*COLD	-0.0230* (0.0104)	-0.0229* (0.0104)	-0.0194* (0.0086)	-0.0195* (0.0086)	-0.0196* (0.0086)	-0.0195* (0.0086)
MOLD	-0.0315** (0.0092)	-0.0332*** (0.0075)	-0.0330*** (0.0075)	-0.0340*** (0.0072)	-0.0343*** (0.0072)	-0.0331*** (0.0070)
ED*MOLD	-0.0047 (0.0150)					
Black	0.0062 (0.0476)	0.0033 (0.0469)	0.0031 (0.0468)	0.0121 (0.0423)	0.0088 (0.0417)	
P399	-0.0842 (0.1553)	-0.0722 (0.1499)	-0.0692 (0.1496)	-0.0806 (0.1479)	-0.0851 (0.1479)	
Density	0.0071 (0.0043)	0.0075 (0.0040)	0.0076 (0.0040)	0.0069 (0.0037)	0.0075* (0.0035)	0.0089*** (0.0025)
Over65	-0.0723 (0.1755)	-0.0759 (0.1752)	-0.0776 (0.1749)			
Noncitizen	0.0487 (0.1637)	0.0372 (0.1595)	0.0372 (0.1591)	0.0634 (0.1478)		

Significance codes: * <0.05, ** <0.01, *** <0.001

3.1.2 Covariance Structure

So far, all models have assumed unstructured covariance structure for $\boldsymbol{G}$ and heterogeneous autoregressive covariance structure for $\boldsymbol{R}$. As previously mentioned, unstructured is the most general and requires fitting the most parameters of all the covariance structures. But since we consider only the intercept as a random effect, $\boldsymbol{G}$ is a scalar and represents the variance of the random intercept. So we fix $\boldsymbol{G}$ as unstructured throughout the analysis. However, we considered different covariance structures for $\boldsymbol{R}$, specifically Variance Components (VC), which assumes uncorrelated errors, Autoregressive (AR(1)), which allows correlated errors and assumes correlations decrease exponentially with increasing time lags, Heterogeneous Autoregressive (ARH(1)), which in analogous to AR(1) except it allows variances on the main diagonal to vary, and finally Antedependence (ANTE(1)), which generalizes

ARH(1) by allowing unique autoregressive parameters for each time lag. The fixed effects parameter estimates for Models A and B for each of these covariance structures are shown in Table 3.4.

Table 3.4: Fixed Effects Estimates for Some Covariance Structures (REML)

(a) Model A

	VC	AR(1)	ARH(1)	ANTE(1)
Intercept	-0.5123 (0.4133)	-0.5153 (0.4165)	-0.0323 (0.2900)	-0.0005 (0.2968)
ED	0.0035 (0.0133)	0.0035 (0.0134)	0.0108 (0.0099)	0.0108 (0.0102)
Time	-0.0080*** (0.0005)	-0.0081*** (0.0005)	-0.0068*** (0.0004)	-0.0081*** (0.0005)
COLD	-0.0396*** (0.0067)	-0.0402*** (0.0070)	-0.0274*** (0.0064)	-0.0237*** (0.0065)
ED*COLD	-0.0138 (0.0080)	-0.0130* (0.0082)	-0.0203* (0.0090)	-0.0189* (0.0091)
MOLD	-0.0238* (0.0116)	-0.0232 (0.0116)	-0.0356*** (0.0081)	-0.0420*** (0.0083)
Female	1.6607* (0.7762)	1.6620* (0.7822)	0.8263 (0.5447)	0.8905 (0.5573)
P399	-0.0117 (0.2000)	-0.0027 (0.2016)	-0.2469 (0.1404)	-0.3356* (0.1437)
AIC	-1526.7	-1533.5	-2515.8	-2530.0
BIC	-1522.9	-1527.7	-2444.3	-2394.8
-2RLL	-1530.7	-1539.5	-2589.8	-2670.0
Parameters	1	2	34	65

(b) Model B

	VC	AR(1)	ARH(1)	ANTE(1)
Intercept	0.2864*** (0.0332)	0.2875*** (0.0336)	0.2698*** (0.0235)	0.2980*** (0.0248)
ED	-0.0032 (0.0130)	0.0032 (0.0131)	0.0064 (0.0096)	0.0066 (0.0101)
Time	-0.0080*** (0.0005)	-0.0081*** (0.0005)	-0.0068*** (0.0004)	-0.0079*** (0.0005)
COLD	-0.0396*** (0.0067)	-0.0402*** (0.0070)	-0.0279*** (0.0064)	-0.0244*** (0.0065)
ED*COLD	-0.0138 (0.0080)	-0.0130 (0.0082)	-0.0197* (0.0090)	-0.0187* (0.0091)
MOLD	-0.0244* (0.0107)	-0.0239* (0.0108)	-0.0331*** (0.0074)	-0.0366*** (0.0078)
Density	0.0104** (0.0039)	0.0102* (0.0039)	0.0089** (0.0027)	0.0090** (0.0028)
AIC	-3495.4	-3498.5	-5157.5	-5230.3
BIC	-3491.5	-3492.7	-5089.9	-5102.8
-2RLL	-3499.4	-3504.5	-5227.5	-5362.3
Parameters	1	2	34	65

We saw that, for Model A, the AIC was minimized for ANTE(1) and the BIC was minimized for AR(1), and for Model B, the AIC and BIC were both minimized for the ANTE(1) covariance structure. However, ANTE(1) requires estimating 33 more parameters than the ARH(1) structure, and many of these parameters are not significant. Further, Yanosky has noted that the "literature suggests that information criteria are not very accurate in selecting the correct covariance model among a set of possible candidate models" [28]. Yanosky found that the AIC and BIC selected the correct model only about half of the time, and that information criteria became "less and less accurate as the true model became more complex." For these reasons, we selected the simpler heterogeneous covariance structure, ARH(1), as the structure

for $\boldsymbol{R}$ in the final model. The parameter estimates, standard errors, and p-values for the final Model A and Model B are shown in Table 3.5.

Table 3.5: Final Model (REML)

	Model A			Model B		
Variable	Est.	S.E.	p-value	Est.	S.E.	p-value
Intercept	-0.0323	0.2900	0.9119	0.2698	0.0235	<.0001
ED	0.0108	0.0099	0.2809	0.0064	0.0096	0.5117
Time	-0.0068	0.0004	<.0001	-0.0068	0.0004	<.0001
COLD	-0.0274	0.0064	<.0001	-0.0279	0.0064	<.0001
ED*COLD	-0.0203	0.0090	0.0245	-0.0197	0.0090	0.0291
MOLD	-0.0356	0.0081	<.0001	-0.0331	0.0074	<.0001
Female	0.8263	0.5447	0.1363			
P399	-0.2469	0.1404	0.0853			
Density				0.0089	0.0027	0.0018

Now, the variance of the random intercept ($\boldsymbol{G}$) in the final model fitted using REML is 0.000424 for Model A and 0.000361 for Model B. The ARH(1) $\boldsymbol{R}$ matrix is of the following form:

$$\begin{bmatrix} \hat{\sigma_1}^2 & \hat{\sigma_1}\hat{\sigma_2}\hat{\rho} & \hat{\sigma_1}\hat{\sigma_3}\hat{\rho}^2 & \dots & \hat{\sigma_1}\hat{\sigma_t}\hat{\rho}^{t-1} \\ & \hat{\sigma_2}^2 & \hat{\sigma_2}\hat{\sigma_3}\hat{\rho} & \dots & \hat{\sigma_2}\hat{\sigma_t}\hat{\rho}^{t-2} \\ & & \hat{\sigma_3}^2 & \dots & \hat{\sigma_3}\hat{\sigma_t}\hat{\rho}^{t-3} \\ & & & \ddots & \vdots \\ & & & & \hat{\sigma_t}^2 \end{bmatrix}$$

The covariance parameter estimates for Models A and B are shown in Table 3.6.

Table 3.6: Covariance Parameter Estimates

(a) Model A

$\hat{\sigma}_1^2 = 0.1016$	$\hat{\sigma}_2^2 = 0.008836$	$\hat{\sigma}_3^2 = 0.01262$	$\hat{\sigma}_4^2 = 0.009199$	$\hat{\sigma}_5^2 = 0.009291$
$\hat{\sigma}_6^2 = 0.004799$	$\hat{\sigma}_7^2 = 0.01086$	$\hat{\sigma}_8^2 = 0.006226$	$\hat{\sigma}_9^2 = 0.007712$	$\hat{\sigma}_{10}^2 = 0.004305$
$\hat{\sigma}_{11}^2 = 0.005025$	$\hat{\sigma}_{12}^2 = 0.2008$	$\hat{\sigma}_{13}^2 = 0.007265$	$\hat{\sigma}_{14}^2 = 0.01595$	$\hat{\sigma}_{15}^2 = 0.01064$
$\hat{\sigma}_{16}^2 = 0.007521$	$\hat{\sigma}_{17}^2 = 0.005193$	$\hat{\sigma}_{18}^2 = 0.003498$	$\hat{\sigma}_{19}^2 = 0.005104$	$\hat{\sigma}_{20}^2 = 0.005032$
$\hat{\sigma}_{21}^2 = 0.01005$	$\hat{\sigma}_{22}^2 = 0.006586$	$\hat{\sigma}_{23}^2 = 0.05684$	$\hat{\sigma}_{24}^2 = 0.009682$	$\hat{\sigma}_{25}^2 = 0.009612$
$\hat{\sigma}_{26}^2 = 0.01025$	$\hat{\sigma}_{27}^2 = 0.009766$	$\hat{\sigma}_{28}^2 = 0.01168$	$\hat{\sigma}_{29}^2 = 0.01096$	$\hat{\sigma}_{30}^2 = 0.07219$
$\hat{\sigma}_{31}^2 = 0.05344$	$\hat{\sigma}_{32}^2 = 0.08435$	$\hat{\sigma}_{33}^2 = 0.03944$	$\hat{\sigma}_{34}^2 = 0.02903$	$\hat{\sigma}_{35}^2 = 0.02885$
$\hat{\rho} = 0.1414$				

(b) Model B

$\hat{\sigma}_1^2 = 0.1014$	$\hat{\sigma}_2^2 = 0.009090$	$\hat{\sigma}_3^2 = 0.01242$	$\hat{\sigma}_4^2 = 0.009001$	$\hat{\sigma}_5^2 = 0.009200$
$\hat{\sigma}_6^2 = 0.004738$	$\hat{\sigma}_7^2 = 0.01084$	$\hat{\sigma}_8^2 = 0.006119$	$\hat{\sigma}_9^2 = 0.007650$	$\hat{\sigma}_{10}^2 = 0.004335$
$\hat{\sigma}_{11}^2 = 0.005205$	$\hat{\sigma}_{12}^2 = 0.2003$	$\hat{\sigma}_{13}^2 = 0.007297$	$\hat{\sigma}_{14}^2 = 0.01619$	$\hat{\sigma}_{15}^2 = 0.01065$
$\hat{\sigma}_{16}^2 = 0.007605$	$\hat{\sigma}_{17}^2 = 0.007605$	$\hat{\sigma}_{18}^2 = 0.003618$	$\hat{\sigma}_{19}^2 = 0.005087$	$\hat{\sigma}_{20}^2 = 0.005071$
$\hat{\sigma}_{21}^2 = 0.009930$	$\hat{\sigma}_{22}^2 = 0.006576$	$\hat{\sigma}_{23}^2 = 0.05647$	$\hat{\sigma}_{24}^2 = 0.009654$	$\hat{\sigma}_{25}^2 = 0.009485$
$\hat{\sigma}_{26}^2 = 0.009953$	$\hat{\sigma}_{27}^2 = 0.009655$	$\hat{\sigma}_{28}^2 = 0.01164$	$\hat{\sigma}_{29}^2 = 0.01073$	$\hat{\sigma}_{30}^2 = 0.07254$
$\hat{\sigma}_{31}^2 = 0.05342$	$\hat{\sigma}_{32}^2 = 0.08419$	$\hat{\sigma}_{33}^2 = 0.03949$	$\hat{\sigma}_{34}^2 = 0.02907$	$\hat{\sigma}_{35}^2 = 0.02909$
$\hat{\rho} = 0.1395$				

3.2 Observations

After accounting for the multicollinearity introduced by correlations between the Female and Density as well as the Female and Black variables, we found that population density was significantly related to COVID-19 growth rate, where an increase in population density was associated with an increase in the average COVID-19 growth rate, given other variables were held constant (p=0.0018). Proportion of Black population and percent of Female population were each positively related to COVID-19 growth rate when considered alone each model (p=0.0568 and p=0.0343, respectively), but strong evidence for significance of these relationships decreased when considering other covariates in the models. Similarly, the percentage of the population between 200 and 399% of the poverty line was negatively related to the COVID-19 growth rate when considered alone in the model (p=0.0210), suggesting that states with higher proportion of middle-income population is associated with lower COVID-19 case growth rate. We also saw that COVID-19 growth rates were decreasing over time during the study period. After considering heterogeneous covariance structures, we found strong evidence that an increase in the average number of lockdown policies (between-state lockdown effect) was associated with a decrease in average COVID-19 growth rate, given other variables are held constant (p<0.0001). After taking into account correlations between daily observations, we found that the within-state lockdown policy effect was also significantly negatively related to COVID-19 (p<0.0001), along with its interaction with the ED variable (p=0.0245 for Model A, p=0.0291 for Model B), meaning that the within-state other lockdown policy effect depended on whether a state declared a state of emergency before or after the national emergency declaration date. For example, as shown in the interaction plots

in Figure 3.3, the estimated average case growth rate for model A when Time=18, MOLD=3.154, Female=0.508, and P399=0.287 is given by

$$\hat{y}_{ij} = 0.0819 - 0.0274COLD_{ij} + \hat{u}_{0i} \text{ when } ED_i = 0$$
$$\hat{y}_{ij} = 0.0927 - 0.0477COLD_{ij} + \hat{u}_{0i} \text{ when } ED_i = 1$$

where $\hat{u}_{0i}$ is the estimated random intercept for the ith state. Similarly, for model B, the estimated average case growth rate when Time=18, MOLD=3.154, and Density=4.653 is given by

$$\hat{y}_{ij} = 0.0844 - 0.0279COLD_{ij} + \hat{u}_{0i} \text{ when } ED_i = 0$$
$$\hat{y}_{ij} = 0.0908 - 0.0476COLD_{ij} + \hat{u}_{0i} \text{ when } ED_i = 1.$$

In other words, the estimated mean of COVID-19 case growth rate at the baseline was higher in states that issued statewide emergency declarations earlier than at the national level, and the within-state effectiveness of other lockdown policies was found to have a greater impact on reducing the COVID-19 case growth rate in these proactive states than states that delayed declarations of emergency.

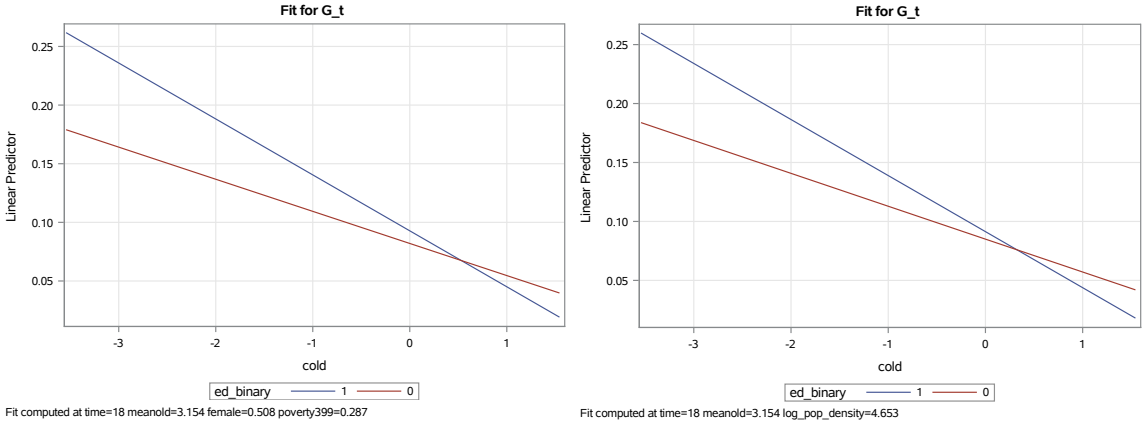

(a) Model A **(b) Model B**

Figure 3.3: Interaction Effect Between ED and COLD

CHAPTER 4

CONCLUSION

4.1 Discussion

Some important contributions of this study include highlighting the difference in COVID-19 outcomes between states that responded proactively and states that responded reactively to the pandemic, disaggregating other lockdown policies into within and between state effects, and adjusting for demographic variables. Comparing proactive and reactive states revealed a significant difference between the two groups in terms of the baseline growth rate and the within-state lockdown policy effectiveness. Disaggregating lockdown policies into between-state and within-state effects revealed that the COVID-19 case growth rate was lower for states that implemented a larger number of lockdown policies on average and the case growth rate was lower when a given state implemented more lockdown policies, relative to its own mean number of lockdown policies. Adjusting for demographic variables allowed us to control for variables that the literature has suggested could be confounding effects in COVID-19 outcomes.

We found that an increase in the average number of other lockdown policies is related to decreasing COVID-19 growth rates, which is consistent with other results that suggest early policy implementation is effective in reducing the spread of COVID-19, since implementing more policies earlier increases the mean number

of other lockdown policies during the study period. We also found that increasing logarithm of the population density is associated with increasing COVID-19 growth rates. This agrees with Hamidi et al.'s initial expectation that increased population density leads to increased person-to-person contacts, which is conducive to the spread of COVID-19, but disagrees with the surprising results of Hamidi et al.'s study [22]. The study, however, considered a longer study period, and Hamidi et al. claims that "compact areas also have the infrastructure to more effectively put in place measures that foster social distancing," so perhaps the study captured the positive effects of this infrastructure that became apparent after the initial lockdown period. Although not quite significant at $\alpha = 0.05$, we found a positive relationship between percent Black population and COVID-19 growth rate, which agrees with other studies that have shown significant relationships between percent of Black population and COVID-19 infection rates [22], though this relationship appears to become insignificant after controlling for population density. We also found that states with larger female populations were associated with increased case growth rates, which is consistent with Pan's finding that the COVID-19 case rate was slightly higher for women than for men. We found that states with larger proportions of middle-income population were associated with decreased case growth rate, but that neither the proportion of state population over the age of 65 nor the proportion non-citizen was significantly related to the case growth rate.

4.2 Limitations

A limitation of this study, as noted by Pan et al. [19], along with essentially all retrospective COVID-19 policy studies, is its ability to find relationships between

the implementation of specific policies and the number of confirmed cases, as the government implemented many policies very close together in time, and the design of the study makes causal inference impossible. This limitation exists for essentially all retrospective COVID-19 policy studies, including the one discussed in this thesis. Further, in order to to look at the effects of lockdown policies alone, we had to restrict the study period to a short window of time, only about a month long, since West Virginia's first confirmed case occurred on March 18, 2020, and states started to implement reopening policies on April 20, 2020. While this allowed us to isolate the effects of lockdown policies from the effects of reopening policies, it reduced the number of samples (days) we could collect from each state. Unfortunately, this choice also restricted access to information about early growth rates and policy effects in states which were affected by and responded to COVID-19 outbreaks earlier than March 16, for example, Washington, which reported its first case on January 21, 2020 and declared a state of emergency on February 29, 2020. Another limitation of this study is that the way we defined the other lockdown policy variable makes it impossible to see the effects of individual types of policies, for example, to determine if stay-at-home orders are more or less effective in controlling the pandemic than school closures. Another possible limitation arises from using a mixed-effects linear model with time-varying covariate. Howard notes that, if the "time-varying covariate itself changes systematically over time," ignoring this systematic change can result in biased estimates of within-subject and between-subject effects [14]. Alternatively, we can consider another time-varying effect model (TVEM) [27].

REFERENCES

[1] Demographics and the economy, 2020. Last accessed 9 March 2023.

[2] Historical apportionment data map, 2020. Last accessed 7 December 2022.

[3] The covid tracking project, 2021. Last accessed 19 March 2023.

[4] Notice on the continuation of the national emergency concerning the coronavirus disease 2019 (covid-19) pandemic, 2023. Last accessed 19 February 2023.

[5] Who coronavirus (covid-19) dashboard, 2023. Last accessed 12 February 2023.

[6] Berman A.E., Miller D.D., Rahn D.W., Hess D.C., Thompson M.A., Mossialos E.A., and Waller J.L. A county-level analysis of socioeconomic and clinical predictors of covid-19 incidence and case-fatality rates in georgia, march-september 2020. *Public Health Reports*, 136(5):626–635, 2021.

[7] P. J. Curran and D. J. Bauer. The disaggregation of within-person and between-person effects in longitudinal models of change. *Annual Review of Psychology*, 62(1):583–619, 2011.

[8] T. Dey, J. Lee, S. Chakraborty, K. Zhang, A. Bhaskar, and F. Dominici. Lag time between state-level policy interventions and change points in covid-19 outcomes in the united states. *Patterns (New York, N.Y.)*, 2(8):100306, 2021.

[9] W. Holmes Finch and Maria E. Hernández Finch. Poverty and covid-19: Rates of incidence and deaths in the united states during the first 10 weeks of the pandemic. *Frontiers in Sociology*, 5, 2020.

[10] L. Guerin and W. Stroup. A simulation study to evaluate proc mixed analysis of repeated measures data. *Conference on Applied Statistics in Agriculture*, 2000.

[11] F.N. Gumedze and T.T. Dunne. Parameter estimation and inference in the linear mixed model. *Linear Algebra and its Applications*, 435(8):1920–1944, 2011.

[12] M. Gurka. Selecting the best linear mixed model under reml. *The American Statistician*, 60(1):19–26, 2006.

[13] C. R. Henderson. Estimation of genetic parameters (abstract). *Annals of Mathematical Statistics*, 21:309–310, 1950.

[14] A. Howard. Leveraging time-varying covariates to test within- and between-person effects and interactions in the multilevel linear model. *Emerging Adulthood*, 3(6):400–412, 2015.

[15] S. Lee, J. Yeo, and C. Na. Learning before and during the covid-19 outbreak: A comparative analysis of crisis learning in south korea and the us. *International Review of Public Administration*, 25(4):243–260, 2020.

[16] R. Littell, G. Milliken, W. Stroup, R. Wolfinger, and O. Schabenberger. *SAS for Mixed Models*. SAS Institute Inc., 2006.

[17] S.G. Luke. Evaluating significance in linear mixed-effects models in r. *Behavior Research Methods*, 49:1494–1502, 2017.

[18] A. Migone. The influence of national policy characteristics on covid-19 containment policies: a comparative analysis. *Policy Design and Practice*, 3(3):259–276, 2020.

[19] A. Pan, L. Liu, C. Wang, H. Guo, X. Hao, Q. Wang, J. Huang, N. He, H. Yu, X. Lin, S. Wei, and T. Wu. Association of public health interventions with the epidemiology of the covid-19 outbreak in wuhan, china. *Journal of the American Medical Association*, 323(19):1916–1923, 2020.

[20] J. Raifman, K. Nocka, D. Jones, J. Bor, S. Lipson, J. Jay, and P. Chan. Covid-19 us state policy database, 2022. Last accessed 28 November 2022.

[21] G. K. Robinson. That blup is a good thing: The estimation of random effects. *Statistical Science*, 6(1):15–32, 1991.

[22] Hamidi S., R. Ewing, and S. Sabouri. Longitudinal analyses of the relationship between development density and the covid-19 morbidity and mortality rates: Early evidence from 1,165 metropolitan counties in the united states. *Health Place*, 64:102378, 2020.

[23] G. Schaalje, J. McBride, and G. Fellingham. Approximations to distributions of test statistics in complex mixed linear models using sas proc mixed. *Statistics, Data Analysis, and Data Mining*, 2001.

[24] Mude W., Oguoma VM., Nyanhanda T., Mwanri L., and Njue C. Racial disparities in covid-19 pandemic cases, hospitalisations, and deaths: A systematic review and meta-analysis. *Journal of Global Health*, 11, 2021.

[25] R.L. Wasserstein and N.A. Lazar. The asa statement on p-values: Context, process, and purpose, the american statistician. *The American Statistician*, 70(2):129–133, 2016.

[26] R. Wolfinger. Heterogeneous variance: Covariance structures for repeated measures. *Journal of Agricultural Biological and Environmental Statistics*, 1(2):205–230, 1996.

[27] T. Xianming. A time-varying effect model for intensive longitudinal data. *Psychological methods*, 17(1):61–77, 2012.

[28] D. J. Yanosky. *Comparability of Covariance Structures and Accuracy of Information Criteria in Mixed Model Models for Longitudinal Data Analysis*. PhD thesis, The University of Georgia, 2007.

APPENDIX A

SAS CODE

Full Model

```
PROC MIXED DATA=data plot=(boxplot(observed marginal conditional
   subject) STUDENTPANEL(blup noblup));
  CLASS state_name timec ed_binary (ref='0');
  MODEL G_t = ed_binary time ed_binary*time cold ed_binary*cold
   meanold ed_binary*meanold female poverty399 log_pop_density
   over65 noncitizen / solution
        influence(iter=5 effect=state_name) ddfm=kr;
  RANDOM intercept / SUB=state_name TYPE = UN G GCORR;
  REPEATED timec / SUB=state_name type=ARH(1) R RCORR;
RUN;
```

Model A

```
PROC MIXED DATA=data plot=(boxplot(observed marginal conditional
   subject) STUDENTPANEL(blup noblup));
  CLASS state_name timec ed_binary (ref='0');
  MODEL G_t = ed_binary time cold ed_binary*cold meanold female
   poverty399 / noint solution influence(iter=5 effect=state_name)
   ddfm=kr;
  RANDOM intercept / SUB=state_name TYPE = UN G GCORR;
  REPEATED timec / SUB=state_name type=ARH(1) R RCORR;
  store out=MixedModelA;
```

```
RUN;
```

Model B

```
PROC MIXED DATA=data plot=(boxplot(observed marginal conditional
   subject) STUDENTPANEL(blup noblup));
  CLASS state_name timec ed_binary (ref='0');
  MODEL G_t = ed_binary time cold ed_binary*cold meanold log_pop_
   density / solution
       influence(iter=5 effect=state_name) ddfm=kr;
  RANDOM intercept / SUB=state_name TYPE = UN G GCORR;
  REPEATED timec / SUB=state_name type=ARH(1) R RCORR;
  store out=MixedModelB;
RUN;
```

Model A Interaction Plot

```
PROC PLM RESTORE=MixedModelA noinfo;
   EFFECTPLOT SLICEFIT(x=cold sliceby=ed_binary);
RUN;
```

Model B Interaction Plot

```
PROC PLM RESTORE=MixedModelB noinfo;
   EFFECTPLOT SLICEFIT(x=cold sliceby=ed_binary);
RUN;
```

APPENDIX B

RESIDUAL PLOTS

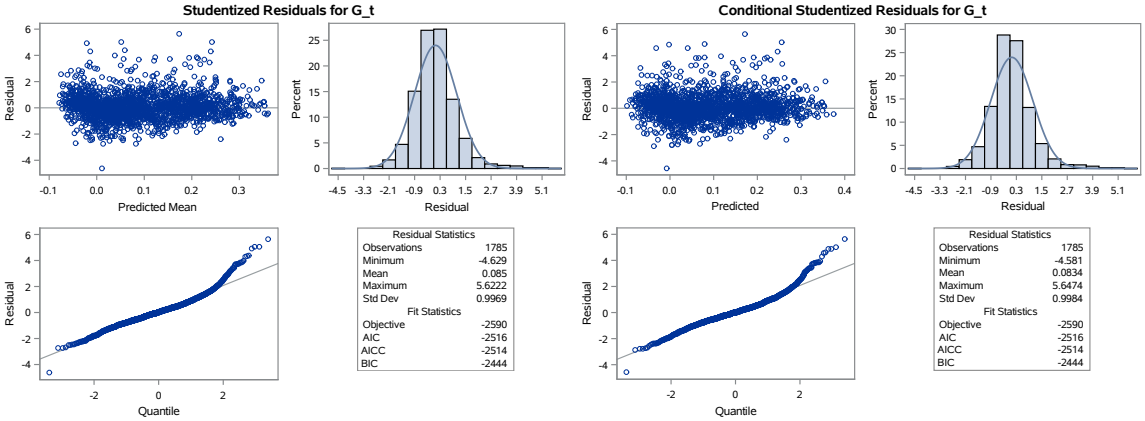

(a) Marginal Studentized Residuals **(b) Conditional Studentized Residuals**

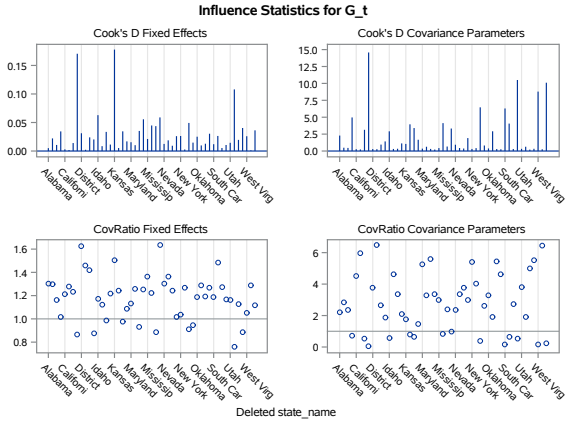

(c) Influence Plots

Figure B.1: Model A

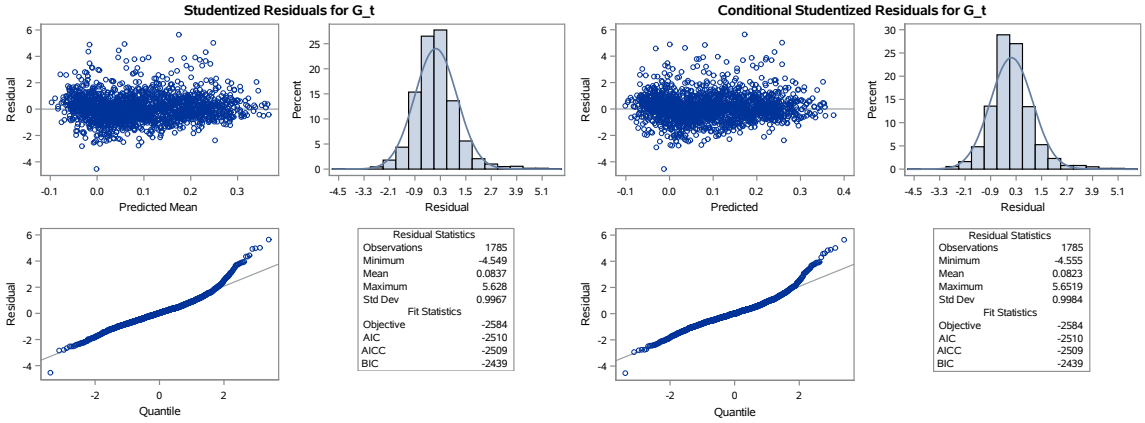

(a) Marginal Studentized Residuals **(b) Conditional Studentized Residuals**

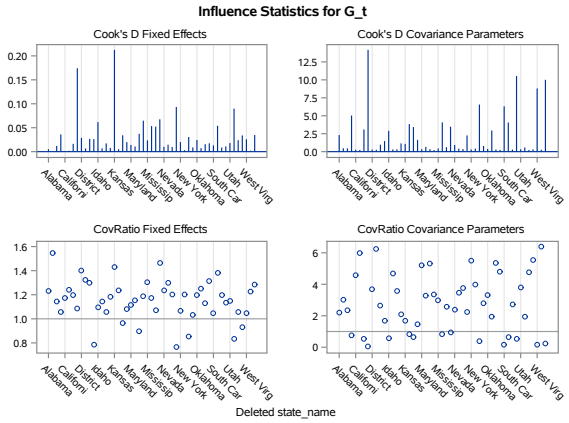

(c) Influence Plots

Figure B.2: Model B